Kinetic Mechanism for the Sequential Binding of Two Single-Stranded Oligodeoxynucleotides to the *Escherichia coli* Rep Helicase Dimer†

Keith P. Bjornson,‡ John Hsieh, Mohan Amaratunga,§ and Timothy M. Lohman*

Department of Biochemistry and Molecular Biophysics, Box 8231, Washington University School of Medicine, 660 South Euclid Avenue, St. Louis, Missouri 63110

Received August 5, 1997; Revised Manuscript Received November 3, 1997

ABSTRACT: *Escherichia coli* Rep helicase is a DNA motor protein that unwinds duplex DNA as a dimeric enzyme. Using fluorescence probes positioned asymmetrically within a series of single-stranded (ss) oligodeoxynucleotides, we show that ss-DNA binds with a defined polarity to Rep monomers and to individual subunits of the Rep dimer. Using fluorescence resonance energy transfer and stopped-flow techniques, we have examined the mechanism of ss-oligodeoxynucleotide binding to preformed Rep dimers in which one binding site is occupied by a single-stranded oligodeoxynucleotide, while the other site is free (P_2S dimer). We show that ss-DNA binding to the P_2S Rep dimer to form the doubly ligated P_2S_2 dimer occurs by a multistep process with the initial binding step occurring relatively rapidly with a bimolecular rate constant of $k_1 = \sim 2 \times 10^6$ M^{-1} s^{-1} [20 mM Tris (pH 7.5), 6 mM NaCl, 5 mM $MgCl_2$, 5 mM 2-mercaptoethanol, and 10% (v/v) glycerol, 4 °C]. A minimal kinetic mechanism is proposed which suggests that the two strands of ss-DNA bound to the Rep homodimer are kinetically distinct even within the P_2S_2 Rep dimer, indicating that this dimer is functionally asymmetric. The implications of these results for the mechanisms of DNA unwinding and translocation by the functional Rep dimer are discussed.

DNA helicases are a class of motor proteins that use energy derived from nucleoside 5′-triphosphate (NTP) binding, hydrolysis, and release of hydrolyzed products (NDP + PO_4^{2-}) to separate duplex DNA into its two complementary single strands and to translocate along the DNA. As such, these enzymes are required in nearly all aspects of DNA metabolism including replication, recombination, and DNA repair (*1*). Furthermore, defects in DNA helicases have recently been implicated as the causative agent of several severe genetic disorders in humans. Xeroderma pigmentosum (XP) is an autosomal recessive disorder that predisposes its victims to cancer and neurological abnormalities due to a deficiency in DNA excision repair. Two of the protein factors comprising the complementation groups, XPB and XPD, posses DNA helicase activity and are components of the general transcription initiation factor TFIIH (*2*). Two other genetic diseases, Cockayne's syndrome and trichothiodystrophy, which both cause developmental and neurological disorders, have complementation groups that also include the helicase subunits of TFIIH (*2*). Bloom's Syndrome, which causes dwarfism, predisposition to cancer, and immunological and behavioral defects, was recently found to be due to a defect in a single gene which is highly homologous to the RecQ helicase of *Escherichia coli* (*3*). In addition, the defective gene that causes the accelerated aging disorder Werner's syndrome encodes an enzyme with DNA helicase activity (*4*, *5*).

Although DNA helicases are of crucial biological importance in all organisms, the mechanisms by which these enzymes function are only beginning to be understood. One of the better characterized helicases is the *E. coli* Rep DNA helicase. Although the Rep protein exists as a monomer (M_r = 76 400) in solution, binding of either single-stranded (ss) or duplex DNA induces it to form a stable dimer (*6*, *7*), and the dimer is active in unwinding DNA (*6*, *8*−*11*). Each subunit of the Rep dimer can bind either ss or double-stranded DNA competitively (*7*). However, a large negative cooperativity accompanies DNA binding to the second subunit of the dimer such that the affinity of DNA for the second subunit is at least 4 orders of magnitude lower than for the first subunit (*7*). Importantly, this negative cooperativity for DNA, and thus the various possible DNA ligation states of the Rep dimer, are modulated allosterically by nucleotide binding (*8*). In the absence of nucleotide, a Rep dimer is favored in which one subunit is bound to ss-DNA, whereas the other subunit is free (a P_2S dimer). However, ADP binding promotes formation of a Rep dimer in which both subunits are bound to ss-DNA (P_2S_2 dimer). Finally, binding of AMPP(NH)P, a nonhydrolyzable ATP analogue, favors a dimer in which both ss- and duplex (D) DNA are bound simultaneously to the dimer, one to each subunit (a P_2SD dimer). Based on these observations, an active, rolling model for DNA unwinding has been proposed in which ATP binding, hydrolysis, and release cycles the Rep dimer through

† This work was supported in part by a grant to T.M.L. from the NIH (GM 45948). K.P.B. received partial support from an NIH training grant (5 T32 GM08492).

* Address correspondence to this author. Tel (314) 362-4393; FAX (314) 362-7183; E-mail lohman@biochem.wustl.edu.

‡ Present address: Department of Biochemistry, Duke University Medical Center, Durham, NC 27710.

§ Present address: General Electric Corp., Research and Development, P.O. Box 8, k-1 Rm 3C30, Schenectady, NY 12301.

S0006-2960(97)01930-2 CCC: $15.00
Published on Web 01/20/1998

a series of conformational states that differ in the relative affinity of the second subunit of the Rep dimer for ss- *vs* ds-DNA (*8*, *12*, *13*). In this model the Rep dimer translocates along DNA by a rolling or subunit switching mechanism and duplex DNA is actively unwound when one subunit of the Rep dimer is bound to the duplex region ahead of the ss/ds-DNA junction.

The doubly ligated Rep dimer, P_2S_2, is a transient high-energy intermediate in the proposed rolling model for DNA unwinding (*8*) and also for Rep dimer translocation along ss-DNA (*11*). Therefore, a detailed characterization of the kinetic mechanism of P_2S_2 formation is necessary to provide further information and tests of these models. Our previous studies showed that the dissociation rate of a fluorescently labeled ss-DNA from the high-affinity site of a P_2S Rep dimer is accelerated by the binding of a second molecule of ss-DNA into the weak binding site in a reaction that transiently forms the P_2S_2 dimer (*11*, *14*). These studies provided a lower limit estimate of $\approx 250-400\ M^{-1}\ s^{-1}$ for the apparent bimolecular rate constant for ss-DNA [$dT(pT)_{15}$] binding to the second subunit of the P_2S Rep dimer to form the P_2S_2 dimer. This lower limit for the apparent bimolecular rate constant is ~10 000-fold lower than that for $dT(pT)_{15}$ binding to the Rep monomer (*14*), and thus we proposed that the actual mechanism of P_2S_2 formation occurs by a multistep process (*14*).

In this report we describe experiments designed to measure directly the initial binding of ss-DNA to the unligated subunit of the P_2S dimer. These experiments show that binding to P_2S occurs by a multistep process with the initial binding step occurring relatively rapidly. Furthermore, the two strands of ss-DNA bound to the Rep homodimer are kinetically distinct, such that the enzymes retains a "memory" of which strand was bound first. The implications of these results for the mechanism of Rep-catalyzed DNA unwinding are discussed.

MATERIALS AND METHODS

Buffers and Rep Protein. Buffers were made with reagent-grade chemicals using distilled H_2O that was deionized using a Milli-Q System (Millipore Corp., Bedford, MA). Binding buffer with Mg^{2+} (BBM buffer) is 20 mM Tris (titrated to pH 7.5 at 4 °C), 6 mM NaCl, 5 mM $MgCl_2$, 5 mM 2-mercaptoethanol, and 10% (v/v) glycerol. Glycerol (spectrophotometric grade) was from Aldrich (Milwaukee, WI). *E. coli* Rep protein was purified to >99% homogeneity as described (*15*) and its concentration was determined spectrophotometrically, using an extinction coefficient for the monomer of $\epsilon_{280} = 7.68 \times 10^4\ M^{-1}\ cm^{-1}$ (*9*).

Oligodeoxynucleotides. Oligodeoxynucleotides were synthesized using an ABI Model 391 automated DNA synthesizer (Applied Biosystems, Foster City, CA) with standard β-cyanoethyl phosphoramidite chemistry. The 2-aminopurine- (2-AP-) containing oligodeoxynucleotides, d[T_5(2-AP)T_4(2-AP)T_5], 5′-d[T_{12}(2AP)T(2AP)T], and 5′-d[T(2AP)T(2AP)T_{12}], were prepared as described (*14*). The $dT(pT)_{15}$ labeled with fluorescein or hexachlorofluorescein was synthesized, deprotected, and purified as described (*10*). The concentrations of the oligodeoxynucleotides were determined by absorbance at 260 nm in 10 mM Tris-HCl (pH 8), 100 mM NaCl, and 1 mM EDTA at 25 °C using extinction coefficients of 115 400 $M^{-1}\ cm^{-1}$ for d[T_5(2-AP)T_4(2-AP)T_5], 5′-d[T_{12}(2AP)T(2AP)T], and 5′-d[T(2AP)T(2AP)T_{12}], 131 240 $M^{-1}\ cm^{-1}$ for 3′F-dT_{16}, 148 790 $M^{-1}\ cm^{-1}$ for 5′HF-dT_{16}, and 129 600 $M^{-1}\ cm^{-1}$ for $dT(pT)_{15}$.

Equilibrium Fluorescence Titrations. Equilibrium fluorescence titrations of the oligodeoxynucleotides containing 2-aminopurine (2-AP) with Rep were performed using an SLM-8100 spectrofluorometer (SLM Instuments Inc., Rochester, NY) in BBM buffer at 4 °C. The excitation wavelength was 315 nm (2 mm slits) and emission fluorescence was monitored at wavelengths > 350 nm using a cut-on filter (2 in. diameter; Oriel Inc., catalog no. 59460,Stratford, CT). After each addition of Rep protein, the sample was stirred with a polyethylene rod and equilibrated for at least 7 min with the shutters closed. A "blank titration" of BBM buffer with Rep was also performed along with each titration of DNA. For each titration point *i*, the corrected fluorescence intensity, F_i, was calculated as $F_i = f_{obs,i} - f_{blank,i}$, where $f_{obs,i}$ and $f_{blank,i}$ are the fluorescence intensities determined for the *i*th point from the actual and blank titrations, respectively. The fraction of the maximal fluorescence enhancement was calculated as $(F_i - F_0)/(F_{max} - F_0)$, where F_0 is the initial fluorescence intensity of DNA samples before addition of Rep and F_{max} is the fluorescence after saturation with Rep. Isotherms obtained from fluorescence titrations were compared graphically with binding isotherms simulated using Scheme 2, the equilibrium constants determined previously (*14*), and the relative 2-AP fluorescence enhancements of the monomer Rep-DNA species, PS and PS*, and the singly ligated Rep dimer, P_2S, reported in Table 1. Simulations and plots were constructed and analyzed using the program KaleidaGraph (Synergy Software, Reading, PA) run on a PowerMac 7200/120.

Fluorescence Stopped-Flow Kinetics. Stopped-flow fluorescence experiments were carried out using an Applied Photophysics SX17MV stopped-flow instrument (Applied Photophysics Ltd., Leatherhead, U.K.) supplied with a 150 W Xe arc lamp. $dT(pT)_{15}$, labeled with fluorescein on its 3′ or 5′ end (dT_{16} -F-3′ and 5-′F-dT_{16}), was excited at 492 nm and its fluorescence emission was monitored at wavelengths > 520 nm using a cut-on filter (Oriel Inc., catalog no. 51300, Stratford, CT). The fluorescence energy transfer experiments were performed by exciting the fluorescein donor (dT_{16} -F-3′) as described above and monitoring the sensitized emission of the hexachlorofluorescein acceptor (5-′HF-dT_{16}) above 610 nm using a cut-on filter (Oriel Inc., catalog no. 51312, Stratford, CT). All of the reported concentrations are the final concentrations in the flow cell after mixing of the reactants.

All reactions were carried out in BBM buffer at 4 °C. The P_2S Rep dimer was preformed by incubating 800 nM Rep monomer with 500 nM oligodeoxynucleotide (syringe concentrations) on ice for at least 5 min. Some of the fluorescent traces were obtained using a logarithmic base time scale (i.e., evenly spaced time points on a logarithmic scale) using the software provided by Applied Photophysics (version 4.22 SX18MV). The utility of sampling data points in this manner is that each phase of a multiphasic time course is well described by an adequate number of data points, which facilitates data analysis. The stopped-flow traces were all obtained in the "oversample" mode so that the instrument collects data at its fastest rate, and then blocks of data are

Scheme 1

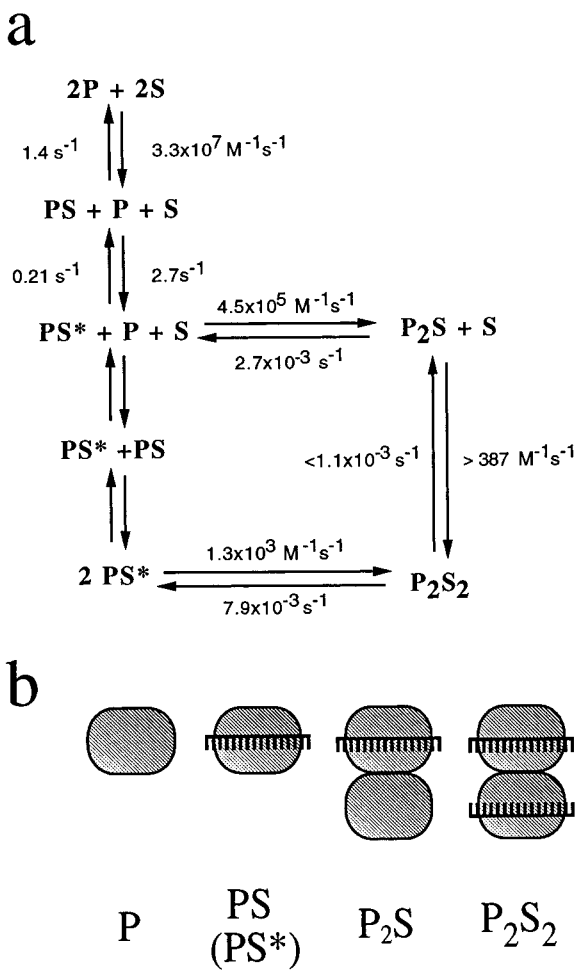

averaged to obtain the individual time points (1000 points/trace). When data are collected using a log time-base the points are not evenly spaced on a linear time scale; hence the signal to noise ratio increases with time since the averaged data blocks are larger at longer times.

Analysis of Kinetic Data. The kinetic time courses were fit to a sum of exponentials as described (*14*) using the software provided with the stopped-flow instrument. The data were plotted using the program KaleidaGraph (Synergy Software, Reading, PA) run on a PowerMac 7500/100.

RESULTS

Our previous studies of the kinetics of short ss-oligodeoxynucleotide ($dT(pT)_{15}$) binding to the Rep monomer, P, and subsequent dimerization to form the singly ligated dimer, P_2S (*14*) have defined the minimal kinetic mechanism shown in Scheme 1. The rate constants shown in Scheme 1 were measured under the same conditions used in the current studies (BBM buffer, 4 °C). These previous studies were performed with the oligodeoxynucleotides $dT(pT)_{15}$ and $d[T_5(2\text{-AP})T_4(2\text{-AP})T_5]$, where 2-AP is the fluorescent nucleotide analogue 2-aminopurine. With 2-AP in the indicated positions within that ss-DNA, there is a 1.7-fold enhancement of the 2-aminopurine fluorescence intensity upon binding to the Rep monomer P and a further 1.4-fold enhancement upon formation of the P_2S dimer (*14*). In addition, the fluorescence properties of the 2-aminopurines embedded within the ss-oligodeoxynucleotide are sensitive to protein conformational changes induced by nucleotide binding and hydrolysis (*11*).

Single-Stranded DNA Binds to Rep with Polarity. DNA helicases generally display a polarity in their DNA unwinding reaction, i.e., they show preference for unwinding duplex DNA possessing either a 3′ or a 5′ ss-DNA flanking the duplex (*16*). This implies that helicases bind to ss-DNA with a defined polarity. As a prelude to the DNA binding experiments described below (monitored using FRET), we first determined whether ss-DNA binds to Rep with a unique orientation with respect to the polarity of the sugar−phosphate backbone. We performed experiments similar to those designed to examine the same question for the phage T4 gene 32 protein (*17*, *18*). Two analogues of $dT(pT)_{15}$ were synthesized, each of which contained 2-aminopurine; however, the positioning of the fluorescent 2-AP was asymmetric within the DNA. One molecule, 5′-dT(2-AP)T-$(2\text{-AP})T_{12}$, has two 2-APs near its 5′ end and the other, 5′-$dT_{12}(2\text{-AP})T(2\text{-AP})T$, has two 2-APs near its 3′ end. The fluorescence intensities (quantum yields) of both molecules, in the absence of Rep, were identical. We performed separate equilibrium titrations of each ss-DNA at three concentrations (200, 300, and 400 nM), with Rep protein while monitoring the change in 2-AP fluorescence. If these oligodeoxynucleotides could bind to Rep in either orientation with respect to the sugar−phosphate backbone, then the extent of the 2-AP fluorescence change is expected to be similar for both molecules. In fact, Figure 1A shows that upon saturation with Rep, the enhancement of the 2-AP fluorescence for each DNA molecule differs significantly, with the ss-DNA containing 2-AP near its 3′ end showing a 5.7-fold enhancement, whereas the ss-DNA with 2-AP near its 5′ end shows only a 1.7-fold enhancement. These results indicate that the Rep dimer binds ss-DNA with a preferred polarity.

Although the midpoints of the three titration curves (shown normalized in Figure 1B) suggest similar affinities of Rep for the three ss-oligodeoxynucleotides, the shapes of the titration curves differ significantly. In fact, these differences in the shapes of the titration curves reflect position-dependent differences in 2-AP fluorescence quantum yield when each ss-oligodeoxynucleotide is bound to the different species of Rep (i.e., PS, PS*, and P_2S). The different final 2-AP fluorescence enhancements shown in Figure 1A clearly indicate that this is the case for the P_2S state. In order to determine the relative 2-AP fluorescence change upon formation of the Rep monomer complexes (PS and PS*), which are only populated transiently during the titration, we performed stopped-flow kinetics experiments (data not shown) as described previously (*14*). Separate stopped-flow experiments were performed by mixing Rep monomer with each ss-DNA (BBM buffer, 4 °C) over a range of protein (100−400 nM) and ss-DNA (0.2 and 1 μM) concentrations. From these independent experiments we determined the relative enhancements of 2-AP fluorescence for each ss DNA bound to Rep monomer (PS + PS*). As listed in Table 1, the relative enhancements of 2-AP fluorescence are 0.75 ± 0.25 and 1.7 ± 0.1 for 3′-end and the 5′-end oligodeoxynucleotides, respectively, compared to a value of 1.7 ± 0.1 for the symmetric oligodeoxynucleotide, $dT_5(2\text{-AP})T_4(2\text{-AP})T_5$ (*14*).

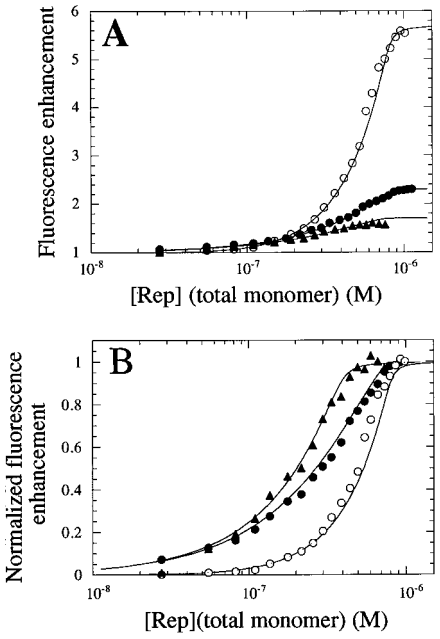

FIGURE 1: Equilibrium binding of 2-aminopurine-modified $dT(pT)_{15}$ to Rep protein, monitored by the enhancement of 2-aminopurine (2-AP) fluorescence. Solutions of $dT(pT)_{15}$ (400 nM), containing 2-AP at various positions within the oligodeoxynucleotide (see Table 1), were titrated with Rep protein at 4 °C in 20 mM Tris-HCl, pH 7.5 at 4 °C, 6 mM NaCl, 5 mM $MgCl_2$, and 10% glycerol (BBM buffer), while the 2-AP fluorescence was monitored (excitation at 315 nm, fluorescence emission monitored at wavelengths > 350 nm). The ss DNA molecules used were (●) "symmetric", 5′-dT_5(2AP)T_4(2AP)T_5; (▲) 2-AP near the 5′-end, 5′dT(2AP)T-(2AP)T_{12}; or (○) 2-AP near the 3′-end, 5′dT_{12}(2AP)T(2AP)T. Fluorescence titrations of 200 and 300 nM ss-DNA with Rep were also performed under the same conditions and identical results were obtained (data not shown). (A) Titrations are plotted as the fluorescence enhancement (relative to free DNA) as a function of total Rep concentration (monomer units). The solid lines are simulated curves based on Scheme 2, using the equilibrium constants $K_1 = 23\ \mu M^{-1}$, $K_2 = 13$, and $K_3 = 170\ \mu M^{-1}$, which were determined previously (*14*), but accounting for the fact that the relative fluorescence enhancement of the three ss-DNA molecules differs when bound to each Rep species (PS/PS* and P_2S) as indicated in Table 1. (B) The three titrations shown in panel A have been replotted after each curve was normalized to its own maximum fluorescence enhancement. The solid lines are simulations based on Scheme 2.

Table 1: Relative 2-Aminopurine Fluorescence Enhancements for the Different Rep-DNA Species

DNA	2-AP position	PS/PS* [a]	P_2S [b]
5′-dT_5(2AP)T_4(2AP)T_5	symmetric	1.7 ± 0.1 [c]	2.4 ± 0.1 [c]
5′-dT_{12}(2AP)T(2AP)T	3′-end	0.75 ± 0.25	5.9 ± 0.2
5′-dT(2AP)T(2AP)T_{12}	5′-end	1.7 ± 0.1	1.7 ± 0.1

[a] Determined from independent stopped-flow experiments as described (*14*). [b] Obtained from the final plateau value of the fluorescence titrations. [c] From Bjornson et al. (*14*).

Scheme 2

$$2P + S \overset{K_1}{\rightleftharpoons} PS + P \overset{K_2}{\rightleftharpoons} PS^* + P \overset{K_3}{\rightleftharpoons} P_2S$$

The very different enhancements of 2-AP fluorescence for the different Rep species bound to the three oligodeoxynucleotides explains the different shapes of the equilibrium fluorescence titrations shown in Figure 1A. The smooth curves overlaying the three titrations shown in Figure 1 were simulated using Scheme 2 with identical values of the equilibrium constants (K_1, K_2, K_3), which had been determined previously for binding of the symmetric oligodeoxynucleotide to Rep (*14*), but accounting for the different relative 2-AP fluorescence enhancements of each ss-DNA when bound to the different Rep species (see Table 1). These simulations suggest that all three oligodeoxynucleotides have the same equilibrium binding affinities, independent of the position of 2-AP within the sequence. The shapes of the isotherms differ only due to the different relative fluorescence changes observed for the different species. These results emphasize the fact that it is essential to know how a spectroscopic signal change correlates with the extent of binding in order to quantitatively interpret a binding titration curve. This is especially true for any system, such as Rep, that undergoes assembly and thus can have multiple oligomeric states, each of which can elicit a difference spectroscopic response upon ligation.

Interestingly, the simulated isotherms shown in Figure 1B indicate that the relative position of the 2-AP within the ss-oligodeoxynucleotide senses the various Rep−DNA states differently. When the 2-AP is near the 5′ end of the ss-DNA, the 2-AP fluorescence enhancement is most sensitive to the first two steps in Scheme 2 (i.e., formation of PS/PS*). However, when 2-AP is positioned near the 3′-end of the ss-DNA, then the 2-AP fluorescence is most sensitive to the second step in Scheme 2 (i.e., dimerization to form P_2S). As previously described (*14*), the ss-DNA containing 2-AP near both ends is sensitive to both processes.

Use of FRET To Measure the Bimolecular Rate Constant for ss-DNA Binding to P_2S. We first attempted to examine the bimolecular binding of a ss-oligodeoxynucleotide to the second subunit of a P_2S dimer by mixing d[T_5(2-AP)T_4(2-AP)T_5] with a preformed P_2S dimer, where S is the nonfluorescent oligodeoxynucleotide $dT(pT)_{15}$, while monitoring changes in 2-aminopurine (2-AP) fluorescence. Although changes in 2-AP fluorescence are observed, these are not sensitive to the bimolecular binding step, but rather conformational changes occurring after binding (data not shown). However, these experiments do provide evidence that binding of ss-DNA to the second site (subunit) on the P_2S dimer is at least a two-step process and provide a lower limit of $\sim 300\ M^{-1}\ s^{-1}$ for the true bimolecular rate constant for binding of ss-DNA to the unligated subunit of P_2S. Therefore, we used a different approach that relies on fluorescence resonance energy transfer (FRET) in order to directly measure the bimolecular step for formation of the doubly ligated P_2S_2 dimer from P_2S. These experiments used two ss-oligodeoxythymidylates, each containing 16 nucleotides: one with a fluorescent donor (fluorescein, F) covalently attached to its 3′ end (dT_{16}-F-3′) and another with a fluorescence acceptor (hexachlorofluorescein, HF) covalently attached to its 5′ end (5′-HF-dT_{16}). We have previously shown that the spectral properties of this donor and acceptor pair are conducive to FRET and have used these to design a sensitive fluorescent assay for DNA unwinding (*10*).

The design of the experiments to directly detect the bimolecular step of ss-DNA binding to the second site within the P_2S dimer is outlined in Scheme 3. We have shown above that ss-DNA binds with polarity to Rep monomers and thus also to each subunit of the dimer. Therefore, if

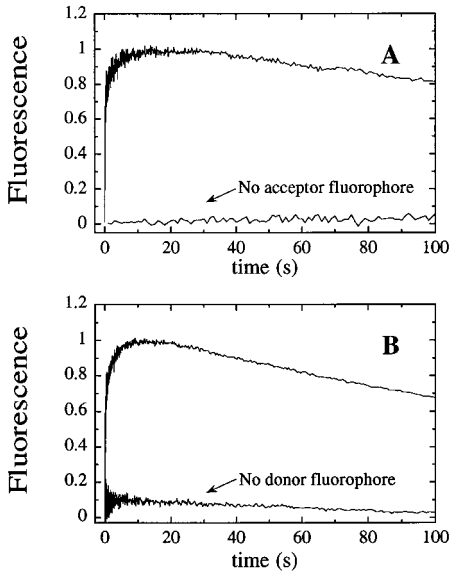

FIGURE 2: Kinetic time course of ss-DNA binding to the P_2S Rep dimer to form a doubly ligated P_2S_2 dimer as monitored by FRET between fluorescein (F) donor and hexachlorofluorescein (HF) acceptor. (A) The P_2S Rep dimer (200 nM) was pre-formed with dT_{16} -F-3′ and mixed in a stopped-flow experiment with either 4 μM 5′-HF-dT_{16} or dT_{16} [no acceptor fluorophore (HF)] as indicated. (B) The P_2S Rep dimer (200 nM) was pre-formed with dT_{16}-F-3′ or dT_{16} (no donor fluorophore) and mixed in a stopped-flow experiment with 2 μM 5′-HF-dT_{16}. All reactions were in BBM buffer at 4.0 °C (λ_{ex} = 494 nm, λ_{em} > 610 nm).

Scheme 3

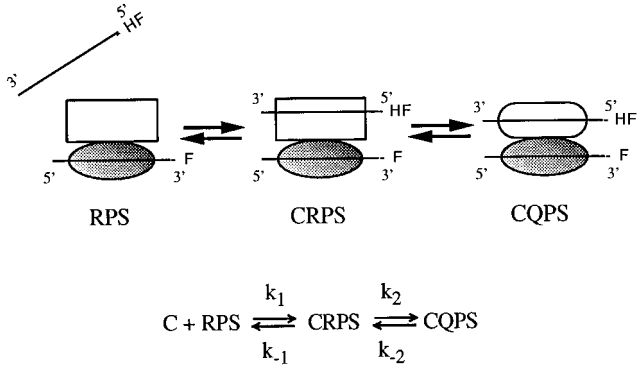

the dimer has an approximate 2-fold symmetry, or if the 3′-end of one bound ss-DNA is near the 5′-end of the second bound ss-DNA in a P_2S_2 complex, and if the ss-DNAs possessing the fluorescence donor/acceptor probes described above are used, then upon formation of the P_2S_2 Rep dimer energy transfer (FRET) from the donor to the acceptor should occur, resulting in an increase in the fluorescence of the acceptor fluorophore. Although the placement of the donor fluorophore at the 3′-end of the ss-DNA and the acceptor at the 5′-end of a separate ss-DNA was based on an assumed C_2 symmetry for the Rep dimer (see Scheme 3), this is not a requirement to observe FRET (see below).

Shown in Figure 2 are fluorescence stopped-flow kinetic traces obtained upon mixing 200 nM P_2S (formed with dT_{16}-F-3′) with an excess of 5′-HF-dT_{16} (4 μM). The donor fluorophore (F) was excited at 494 nm (its maximum excitation wavelength) and the sensitized emission fluorescence from the acceptor fluorophore (HF) was monitored at wavelengths > 610 nm. A biphasic kinetic time course was observed with an increase in fluorescence emission of the

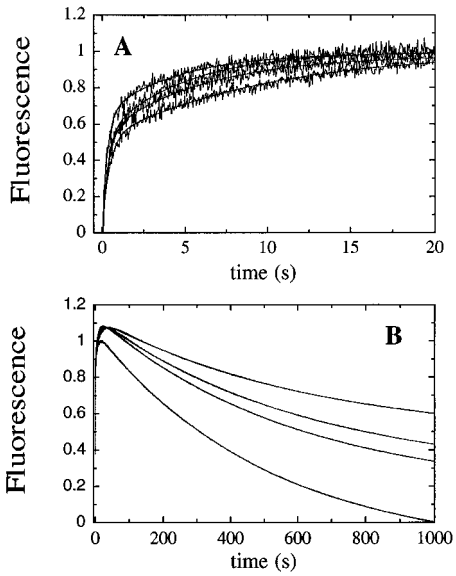

FIGURE 3: Fluorescence resonance energy transfer upon binding of 5′-HF-dT_{16} to a P_2S Rep dimer. (A) The FRET time course (λ_{ex} = 494 nm, $\lambda_{em} \geq$ 610 nm) for the first 20 s as monitored in a stopped-flow experiment upon mixing 200 nM P_2S, preformed with dT_{16}-F-3′ (F is fluorescein donor) with 0.6 (bottom trace), 0.8, 1.0, and 2.0 μM (top trace) 5′HF-dT_{16} (HF is hexachlorofluorescein acceptor) as described in Materials and Methods. (B) The same reactions are shown over 1000 s at 0.6 (top trace), 0.8, 1.0, and 2.0 μM (bottom trace) 5′-HF-dT_{16}. Each time course in both panels was fit to the sum of two exponentials and the fits are overlaid on the data. The apparent rate constants $k_{obs,1}$ and $k_{obs,2}$, obtained from the double-exponential fit to panel A, and $k_{obs,3}$, obtained from the fit to the slow phase in panel B, are plotted in Figure 4.

acceptor (HF), followed by a slow decrease in fluorescence intensity. Also shown in Figure 2 are two control experiments performed under identical conditions except that unmodified dT_{16} was substituted for the fluorescently labeled dT_{16} molecules. These controls show that the observed increase in donor (HF) fluorescence requires the presence of both the donor and acceptor fluorophores and thus originates from a true transfer of energy from the donor (λ_{ex} = 494 nm) to the acceptor fluorophore (λ_{em} > 610 nm) upon formation of the P_2S_2 dimer.

Figure 3 shows fluorescence stopped-flow traces obtained upon mixing 200 nM P_2S (formed with dT_{16}-F-3′) with varying concentrations (0.6 −2 μM) of 5′-HF-dT_{16}. The traces were fit to a sum of three exponential phases and the nonlinear least-square-best fits are overlaid on the data. The observed rate constants for each phase are plotted as a function of excess [5′-HF-dT_{16}] in Figure 4. The fast phase, $k_{obs,1}$, increases linearly with increasing [5′-HF-dT_{16}], whereas the middle rate constant, $k_{obs,2}$, increases with a hyperbolic dependence on [5′-HF-dT_{16}]. The first two phases could be well resolved from the third phase ($k_{obs,3}$) and were analyzed in terms of the two-step binding mechanism shown in Scheme 3.

On the basis of our previous studies (*11*, *19*), the P_2S Rep dimer in Scheme 3 is depicted as asymmetric, i.e., with nonequivalent subunits due to the presence of bound ss-DNA. One subunit contains a weak DNA binding site (rectangle), while the other subunit contains the originally bound DNA in the tight DNA binding site (shaded oval). In the kinetic scheme shown below the cartoon, the initial weak ss-DNA binding site is designated as R and the tight site is designated

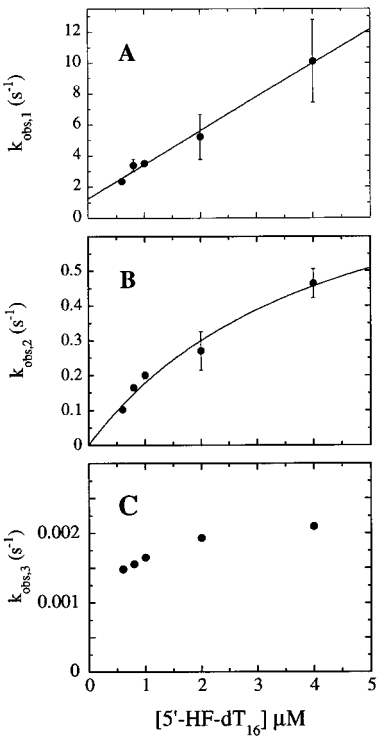

FIGURE 4: Apparent rate constants for 5′HF-dT$_{16}$ binding to the P_2S Rep dimer. (A) Apparent rate constant, $k_{obs,1}$, for the first phase of the time courses shown in Figure 3, reflecting the fast fluorescence enhancement, is plotted as a function of 5′HF-dT$_{16}$ (acceptor) concentration. The data were fit to a straight line with slope = $(2.2 \pm 0.1) \times 10^6$ M^{-1} s^{-1} and an intercept of 1.2 ± 0.3 s^{-1}. (B) Apparent rate constant, $k_{obs,2}$, for the middle phase of the time courses shown in Figure 3, plotted as a function of 5′HF-dT$_{16}$ concentration. The data were fit to a square hyperbola (with intercept constrained to equal zero) with a plateau value of 0.9 ± 0.1 s^{-1} and an apparent K_D of 4 ± 1 μM. (C) Apparent rate constant, $k_{obs,3}$, of the slowest phase of the time courses in Figure 3, plotted as a function of 5′HF-dT$_{16}$ concentration.

as P, the acceptor labeled ss-DNA is designated as C, for competitor, whereas the donor-labeled ss-DNA is designated as S. In Scheme 3, the initial binding event to form the CRPS complex is followed by an isomerization in which the weak site (R) undergoes a conformational change to form the species CQPS, where the Q protomer (squared oval) is a conformational isomer of the weak ss-DNA binding site. On the basis of this model, our data indicate that there is an increase in the fluorescence emission intensity of the acceptor fluorophore upon isomerization of the R subunit to form the Q conformation. The basis for this effect is not known although it could potentially result from some combination of a decrease in the distance between the fluorophore donor and acceptor, a change in their relative orientations or a direct perturbation of the fluorophores upon isomerization.

For the two-step binding mechanism shown in Scheme 3 and under conditions of excess competitor ss-DNA, C, the concentration dependencies of the apparent rate constants $k_{obs,1}$ and $k_{obs,2}$ are given by eqs 1 and 2, respectively (*20*).

$$k_{obs,1} \approx k_1[C] + k_2 + k_{-2} + k_{-1} \quad (1)$$

$$k_{obs,2} \approx \frac{k_1[C](k_2 + k_{-2}) + k_{-1}k_{-2}}{k_1[C] + k_2 + k_{-2} + k_{-1}} \quad (2)$$

By use of eq 1, the apparent bimolecular rate constant, $k_1 = (2.2 \pm 0.1) \times 10^6$ M^{-1} s^{-1}, is obtained from the slope of the line in Figure 4A. This rate constant is considerably larger than our previous lower estimate of 250 M^{-1} s^{-1} obtained from the ss-DNA exchange kinetics with the ss-DNA containing 2-AP (*14*); however, it is still an order of magnitude slower than the apparent bimolecular rate constant measured for binding nearly the same oligodeoxynucleotide to the Rep monomer (*14*). From the intercept of the plot in Figure 4A, we estimate $(k_2 + k_{-2} + k_{-1}) \approx 1.2 \pm 0.3$ s^{-1}. According to eq 2, the plateau value of $k_{obs,2}$, obtained from extrapolation to infinite competitor ss-DNA concentration (Figure 4B), provides an estimate of $(k_2 + k_{-2}) \approx 0.9 \pm 0.1$ s^{-1}. The difference between the intercept in Figure 4A and the plateau value in Figure 4B provides an estimate of the dissociation rate constant, $k_{-1} \approx 0.3 \pm 0.1$ s^{-1}. We note that k_{-1} reflects the dissociation rate constant of ss-DNA from the weak site of the Rep dimer. For comparison, the dissociation rate of ss-DNA from the high-affinity site, i.e., from P_2S, is $\sim 10^{-4}-10^{-5}$ s^{-1}. This large difference in dissociation rate constants is a reflection of the large negative cooperativity for ss-DNA binding to the two sites of the Rep dimer.

As shown in Figure 3B, the fluorescence enhancement of the acceptor fluorophore slowly decays at longer times and the observed rate constant, $k_{obs,3}$, for this third phase is plotted as a function of 5′-HF-dT$_{16}$ concentration in Figure 4C. This slow decrease in fluorescence energy transfer is expected because in the presence of a large excess of ss-DNA, the doubly ligated P_2S_2 Rep dimer is not thermodynamically stable (in the absence of ATP) due to the large negative cooperativity for DNA binding (*14*, *22*) and thus will eventually dissociate to form PS monomers (*11*, *21*), resulting in a loss of FRET due to separation of the donor and acceptor fluorophores. However, as shown previously (*11*), ATP hydrolysis by the P_2S_2 dimer enhances the rate of release of ss-DNA from one subunit of the P_2S_2 Rep dimer, so that ss-DNA dissociation becomes considerably faster than dimer dissociation. Thus, in the presence of ATP, the Rep dimer remains intact during multiple rounds of DNA exchange, which is necessary for processive unwinding and translocation.

Comparison of Kinetics upon Placing the Donor 3′ or 5′ on dT$_{16}$ in the FRET Binding Assay. Our original design of the FRET experiment placed the donor and acceptor fluorophores at the 3′ and 5′ ends of their respective oligodeoxynucleotides (see cartoon in Scheme 3). However, we were also interested to test whether the relative placement of the fluorophores (i.e., at the same or opposite ends of their respective ss-DNA) would influence the kinetics and/or magnitude of the observed fluorescence energy transfer. Shown in Figure 5 is a direct comparison of the binding of 5′-HF-dT$_{16}$ (1 μM) to the P_2S dimer, preformed with either dT$_{16}$-F-3′ or 5′F-dT$_{16}$. Interestingly, the main difference between the two kinetic time courses is the absence of the second phase ($k_{obs,2}$), corresponding to the isomerization step, when both donor and acceptor are on the same 5′-end of the two ss-DNA molecules. However, the rates ($k_{obs,1}$) and amplitudes of the first phases are comparable (see Figure 5A) and the value of $k_{obs,3}$ for the slow fluorescence decay phase is the same within error for both (see Figure 5B). Nevertheless, the fact that the observed FRET changes differ when the fluorescein donor is placed either at the 5′ or 3′

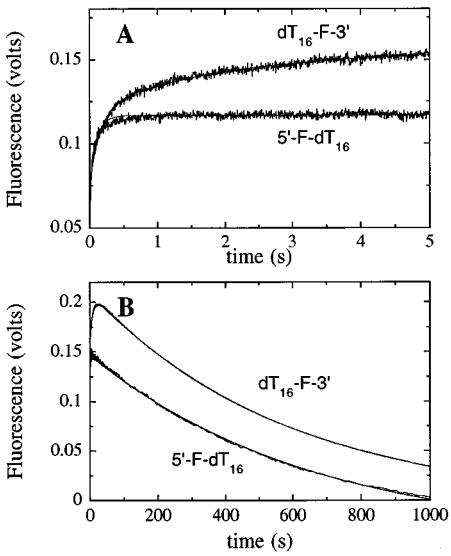

FIGURE 5: Comparison of the time course of FRET observed upon binding 5′-HF-dT_{16} to the P_2S Rep dimer, pre-formed with either dT_{16}-F-3′ or 5′-F-dT_{16}. (A) The first 5 s of two stopped-flow experiments (λ_{ex} = 494 nm, λ_{em} > 610 nm) performed by mixing 5′HF-dT_{16} (1 μM) with P_2S Rep dimer (200 nM), pre-formed with either dT_{16}-F-3′or 5′-F-dT_{16} as indicated. (B) The same reactions as in panel A but monitored for 1000 s. The traces were fit to a sum of three exponentials for the dT_{16}-F-3′ data with $k_{obs,1}$ = 6.5 ± 0.2 s^{-1}, $k_{obs,2}$ =0.52 ± 0.02 s^{-1}, and $k_{obs,3}$ = 0.0015 ± 0.0001 s^{-1}. The fluorescence traces obtained using the 5′-F-dT_{16} were fit to a double exponential with $k_{obs,1}$ = 10.7 ± 0.3 s^{-1} and $k_{obs,2}$ = 0.0017 ± 0.0001s^{-1} (compare with $k_{obs,3}$ for the dT_{16} -F-3′ trace). The fits are overlaid on the data.

end of the ss-DNA bound in P_2S also supports our conclusion that ss-DNA binds to Rep with a preferred "polarity".

DISCUSSION

The experiments reported here demonstrate that ss-DNA binds to the *E. coli* Rep monomer and individual subunits of the functional dimer with a preference for a particular polarity with respect to the sugar−phosphate backbone of the ss-DNA. This is not surprising, in light of the numerous demonstrations of polarity of DNA unwinding observed for most helicases. In fact, such polarity of DNA unwinding must have its basis in the ability of helicases such as Rep to distinguish the orientation of the ss-DNA backbone. This conclusion has recently been supported by X-ray crystal structures of the Rep helicase in complex with a ss-oligodeoxynucleotide, which shows a unique orientation of the ss-oligodeoxynucleotide (*23*).

The kinetic mechanism of ss-DNA ($dT(pT)_{15}$) binding to a preformed P_2S Rep dimer was investigated by fluorescence stopped-flow techniques. The results yield a minimum estimate of (2.2 ± 0.1) × 10^6 M^{-1} s^{-1} for the apparent bimolecular rate constant, k_1, for initial formation of the doubly ligated P_2S_2 complex. This rate constant is much faster than the lower limit of ≈ 250 M^{-1} s^{-1} that we estimated previously from a study of the kinetics of ss-DNA exchange using a 2-aminopurine-labeled oligodeoxynucleotide (*11*). In fact, as we suspected, the overall kinetics of association of ss-DNA to the P_2S dimer is multiphasic, indicating a multistep process. A kinetic mechanism that models the binding of ss-DNA to P_2S as a two-step process is consistent with the fluorescence time courses observed for each probe. On the basis of our previous studies (*11*, *19*), the P_2S Rep dimer is functionally asymmetric with a strong and a weak ss-DNA binding site. Our current results indicate that the initial binding of ss-DNA into the weak site of the P_2S dimer is followed by a conformational change. The apparent rate constant for this isomerization is on the order of ≈0.5 s^{-1}. As always, this minimal kinetic scheme does not preclude the possibility of a more complicated mechanism.

Recent X-ray crystallographic determinations of structures of Rep monomers bound to ss-DNA have suggested a structural basis for the functional asymmetry associated with the Rep dimer (*23*). Within the asymmetric unit of the crystal, two forms of the Rep monomer bound to ss-DNA are observed that differ in the relative orientation of one subdomain (2B) with respect to the remaining three subdomains. These conformations differ by a 130° swiveling of the 2B domain about a hinge region connected to the other three subdomains. These two forms of the Rep monomer are referred to as open vs closed since in one form a cleft into which ss-DNA binds is open, whereas in the other form it is closed. Furthermore, protease studies indicate that the hinge region becomes accessible to cleavage by trypsin upon binding ss-DNA (*23*, *24*). It remains to be determined whether some subset of the open and closed forms of the Rep monomer observed in the crystal structures corresponds to the weak ss-DNA binding conformation and the tight DNA binding conformation, respectively.

The use of Forster resonance energy transfer between the two fluorescent probes, one on each ss-oligodeoxynucleotide, provided a means to measure directly the apparent bimolecular rate constant for ss-DNA binding to the P_2S Rep dimer. Presumably, this is because the FRET assay is sensitive to the relative distances between the donor and acceptor fluorophores and thus is uniquely suited to detect the formation of the doubly ligated P_2S_2 species. Nevertheless, the apparent bimolecular rate constant [k_1 = (2.2 ± 0.1) × 10^6 M^{-1} s^{-1}) for the association of ss-DNA to the P_2S Rep dimer is a factor of ∼10 smaller than the second-order rate constant for binding of a similar oligonucleotide to the Rep monomer under the same conditions (*14*). This suggests the possibility that the apparent second-order rate constant for formation of P_2S_2 may still represent only a lower estimate for the true bimolecular rate constant.

On the basis of our demonstration that ss-DNA binds with a preferred polarity to Rep monomers and subunits of the Rep dimer, the FRET studies reported here were first performed by placing the donor and acceptor fluorophores on the opposite ends (3′ and 5′, respectively) of individual ss-oligodeoxynucleotides. It was reasoned that since each ss-DNA binds with polarity to a Rep subunit (as shown in the cartoon in Scheme 3), this configuration would orient the donor and acceptor pair within a P_2S_2 Rep dimer that possesses C_2 symmetry so that maximum energy transfer could occur. In fact, it was interesting that energy transfer was also observed in a similar set of experiments in which the donor and acceptor fluorophores were both placed on the 5′ end of their respective oligodeoxynucleotides (5′HF-dT_{16} and 5′F-dT_{16}). However, in this case, a lower extent of energy transfer was observed when compared to the experiment performed with the donor and acceptor pair on opposite ends of each oligodeoxynucleotide (see Figure 5B).

The fact that the FRET binding assay differentiates between the relative orientations of the donor and acceptor pair also indicates that the Rep dimer binds ss-DNA with directional bias. Although we do not yet know how the two subunits are oriented within the functional Rep dimer, the recent X-ray structural studies suggest that the relative distances and orientations of the two DNA binding sites within the functional Rep dimer may be able to vary over a wide range due to the potentially large relative movements of protein domains that may occur within a dimer (*23*). This may explain why FRET is observed in a P_2S_2 complex, although to different extents, regardless of whether the acceptor is on the 3′ or the 5′-end of the ss-DNA.

The demonstration that ss-DNA binds to the Rep helicase with a preferred polarity with respect to its sugar-phosphate backbone provides important information for any proposed mechanism of helicase unwinding. Helicases are generally classified with respect to their polarity of DNA unwinding, being either 3′ to 5′ helicases (e.g., Rep, UvrD, SV40 large T antigen) or 5′ to 3′ (e.g., *E. coli* DnaB, T7 gene 4, T4 gene 41), depending on whether unwinding is facilitated by the presence of a covalently attached 3′ or 5′ ss-DNA flanking the duplex (*16*). Any explanation of this polarity of unwinding must be based in the ability of helicases to bind ss-DNA with a preferred polarity.

The kinetic data presented here show that, upon binding of ss-DNA into the weak site of the P_2S dimer to form a P_2S_2 complex, the dimer is still functionally asymmetric since the two molecules of ss-DNA display vastly different dissociation kinetics. Multiple rounds of binding and release in the weak ss-DNA binding site precede the eventual displacement of the ss-DNA originally bound in the tight site of the Rep dimer. These results rule out a model in which the bimolecular binding step is slow (e.g., ≈ 500 M^{-1} s^{-1}) and, upon formation of the P_2S_2 Rep dimer, either strand of ss-DNA would be equally likely to dissociate. Instead, these data demonstrate that the Rep dimer can distinguish which strand of ss-DNA was bound first and preferentially retains that strand upon formation of the seemingly symmetric doubly ligated P_2S_2 dimer. Our previous data have shown that a P_2S Rep dimer, while undergoing ATP hydrolysis, will bind a second (fluorescent) molecule of DNA relatively rapidly ($t_{1/2} \approx 4$ s), as compared to the apparent slow enhancement of 2-AP fluorescence observed in the absence of ATP (*11*). It was proposed that the preexisting tight and weak DNA binding sites interconvert rapidly during ATP hydrolysis, which allows the P_2S dimer to capture a fluorescent competitor ss-DNA upon formation of the P_2S_2 dimer. This is in contrast to a model in which ATP hydrolysis simply accelerates the bimolecular binding step to form P_2S_2 more rapidly. On a long ss-DNA lattice, the Rep dimer should be able to translocate by binding a distal ss-DNA segment into the weak DNA binding site of P_2S, to transiently form the P_2S_2 dimer, and then release the previously bound segment. This process requires the rapid interconversion of the preexisting tight and weak DNA binding sites, and it is this process that seems to be accelerated by ATP hydrolysis (*11*). After this isomerization, the ss-DNA originally bound in the tight site of the P_2S_2 dimer then dissociates from the now low-affinity site, while the newly bound region of ss-DNA remains tightly bound to the other site. This would ensure that the Rep dimer remains bound to at least one segment of ss-DNA at all times, which prevents dissociation of the functional dimer.

The kinetic nonequivalence of the two ss-DNA binding sites of the Rep homodimer may also be relevant to the mechanism of the unwinding reaction. The P_2S_2 dimer characterized in this report is a proposed intermediate following the active unwinding event in the rolling model (*8*). If the dissociation kinetics of both strands of ss-DNA were identical, either ss-DNA segment could be released following the melting of the duplex DNA. Release of the newly generated ss-DNA from the unwinding event would be a backwards step (i.e., the dimer has moved away from the duplex). However, our data show that the ss-DNA strand that is released from the transiently formed P_2S_2 dimer depends upon the path by which the doubly ligated dimer was formed. In this manner, the P_2S_2 Rep dimer could preferentially release the ss-DNA that had been bound to the previous tight site and thus impart a directional bias to the rolling process. Of course, an asymmetry in the nucleotide ligation state of the P_2S_2 dimer may also play a role in identifying the ss-DNA that is to be released from the P_2S_2 dimer. The conformational change within the P_2S_2 dimer that changes the relative affinities of each subunit for ss-DNA, resulting in the release of ss-DNA to regenerate the P_2S dimer, is accelerated by ATP hydrolysis (*11*). The re-formation of the P_2S Rep intermediate is needed to continue the DNA unwinding cycle and the acceleration of this step may be one (of several) central roles for ATP hydrolysis in the unwinding mechanism (*19*).

ACKNOWLEDGMENT

We thank Thang Ho for excellent technical assistance in the synthesis and purification of the oligodeoxynucleotides used in this study and J. Ali and K. Maluf for discussions and a critical reading of the manuscript.

REFERENCES

1. Matson, S. W., Bean, D. W., & George, J. W. (1994) *Bioessays 16*, 13−22.
2. Sancar, A. (1996) *Annu. Rev. Biochem. 65*, 43−81.
3. Watt, P. M., & Hickson, I. D. (1996) *Curr. Biol. 6*, 265−267.
4. Suzuki, N., Shimamoto, A., Imamura, O., Kuromitsu, J., Kitao, S., Goto, M., & Furuichi, Y. (1997) *Nucleic Acids Res. 25*, 2973−2978.
5. Gray, M. D., She, J.-C., Kamath-Loeb, A. S., Blank, A., Sopher, B. L., Martin, G. M., Oshima, J., & Loeb, L. A. (1997) *Nat. Genet. 17*, 100−103.
6. Chao, K., & Lohman, T. M. (1991) *J. Mol. Biol. 221*, 1165−1181.
7. Wong, I., Chao, K. L., Bujalowski, W., & Lohman, T. M. (1992) *J. Biol. Chem. 267*, 7596−7610.
8. Wong, I., & Lohman, T. M. (1992) *Science 256*, 350−355.
9. Amaratunga, M., & Lohman, T. M (1993) *Biochemistry 32*, 6815−6820.
10. Bjornson, K. P., Amaratunga, M., Moore, K. J. M., & Lohman, T. M. (1994) *Biochemistry 33*, 14306−14316.
11. Bjornson, K. P., Wong, I., & Lohman, T. M. (1996) *J. Mol. Biol. 263*, 411−422.
12. Lohman, T. M. (1992) *Mol. Microbiol. 6*, 5−14.
13. Lohman, T. M. (1993) *J. Biol. Chem. 268*, 2269−2272.
14. Bjornson, K. P., Moore, K. J. M., & Lohman, T. M. (1996) *Biochemistry 35*, 2268−2282.
15. Lohman, T. M., Chao, K., Green, J. M., Sage, S., & Runyon, G. (1989) *J. Biol. Chem. 264*, 10139−10147.

16. Lohman, T. M., & Bjornson, K. P. (1996) *Annu. Rev. Biochem. 65*, 169−214.
17. Kelly, R. C., Jensen, D. E., & von Hippel, P. H. (1976) *J. Biol. Chem. 251*, 7240−7250.
18. Giedroc, D. P., Khan, R., & Barnhart, K. (1991) *Biochemistry 30*, 8230−8242.
19. Wong, I., & Lohman, T. M. (1997) *Biochemistry 36*, 3115−3125.
20. Johnson, K. A. (1992) in *The Enzymes*, pp 1−61, Academic Press, Inc., New York.
21. Wong, I., Moore, K. J. M., Bjornson, K. P., Hsieh, J., & Lohman, T. M. (1996) *Biochemistry 35*, 5726−5734.
22. Wong, I., & Lohman, T. M. (1996) *Proc. Natl. Acad. Sci. U.S.A. 93*, 10051−10056.
23. Korolev, S., Hsieh, J., Gauss, G. H., Lohman, T. M., & Waksman, G. (1997) *Cell 90*, 635−647.
24. Chao, K., & Lohman, T. M. (1990) *J. Biol. Chem. 265*, 1067−1076.

BI9719307